

## Electronic Supplementary Information (ESI)

### Annealing-free highly crystalline solution-processed molecular metal oxides for efficient single-junction and tandem polymer solar cells

Maria Vasilopoulou<sup>1,\*</sup>, Ermioni Polydorou<sup>1,2</sup>, Antonios M. Douvas<sup>1</sup>, Leonidas C. Palilis<sup>2</sup>, Stella Kennou<sup>3</sup> and Panagiotis Argitis<sup>1</sup>

<sup>1</sup>*Institute of Nanoscience and Nanotechnology (INN), National Center for Scientific Research “Demokritos”, 15310 Aghia Paraskevi Attikis, Athens, Greece*

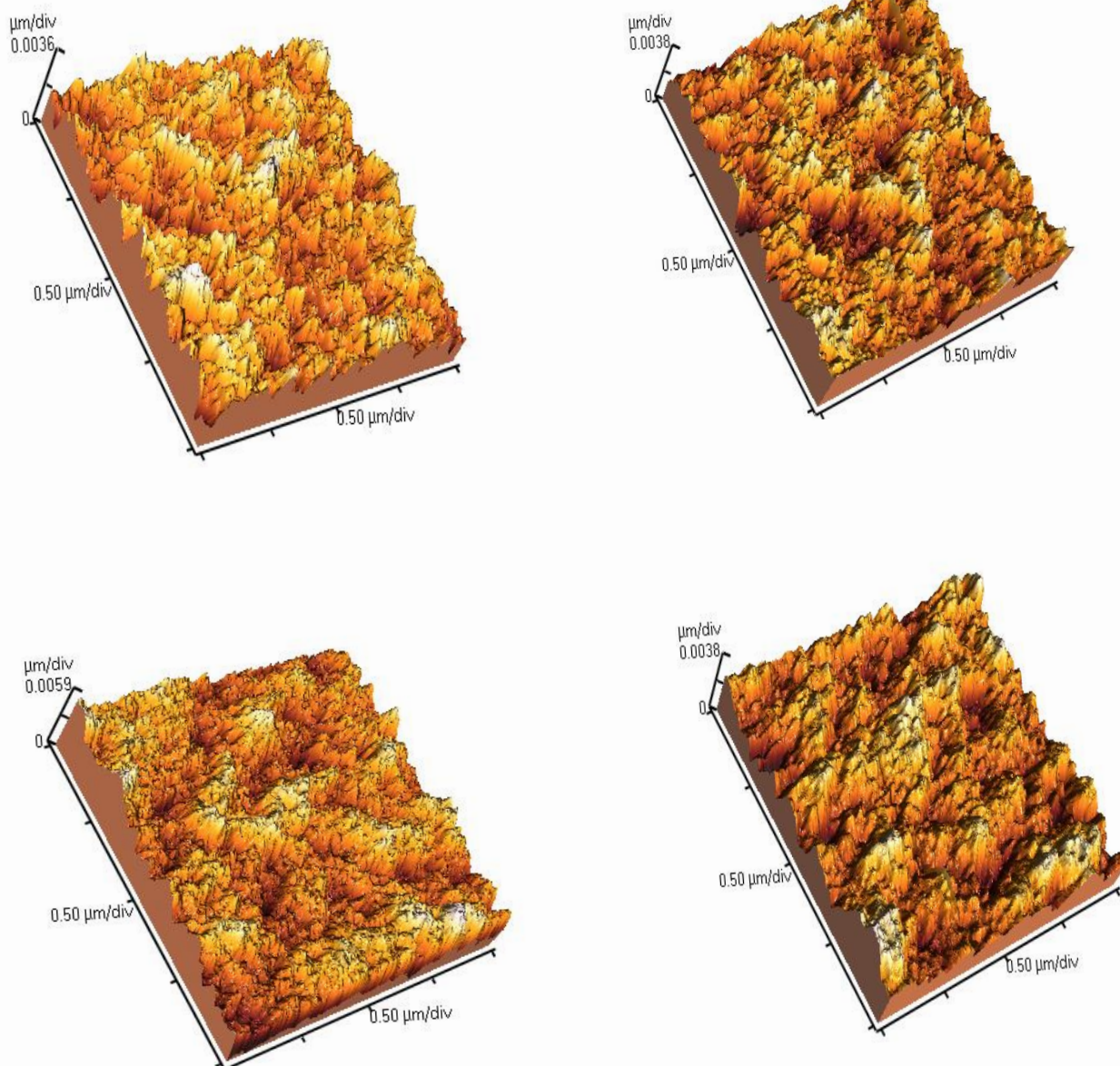
<sup>2</sup>*Department of Physics, University of Patras, 26500 Patras, Greece*

<sup>3</sup>*Department of Chemical Engineering, University of Patras, 26500 Patras, Greece*

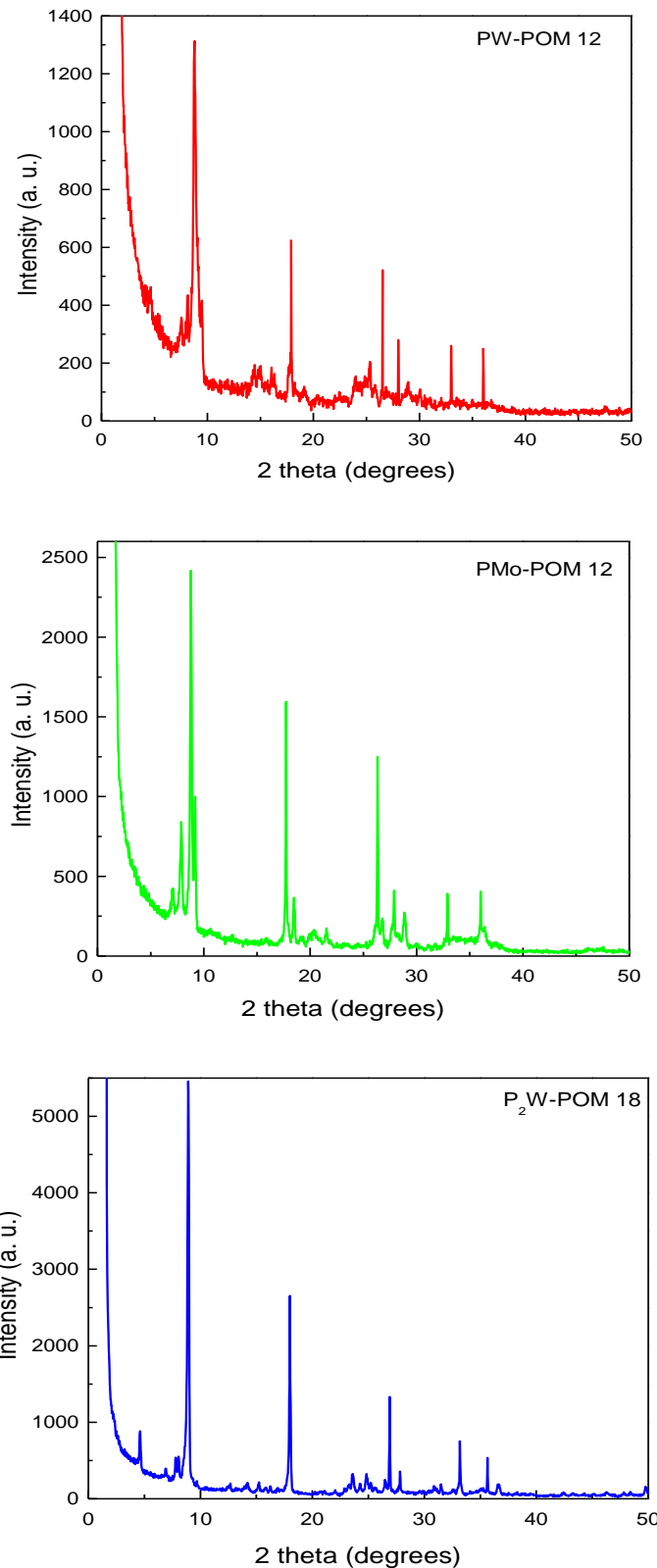
\*email: mariva@imel.demokritos.gr

### Contents

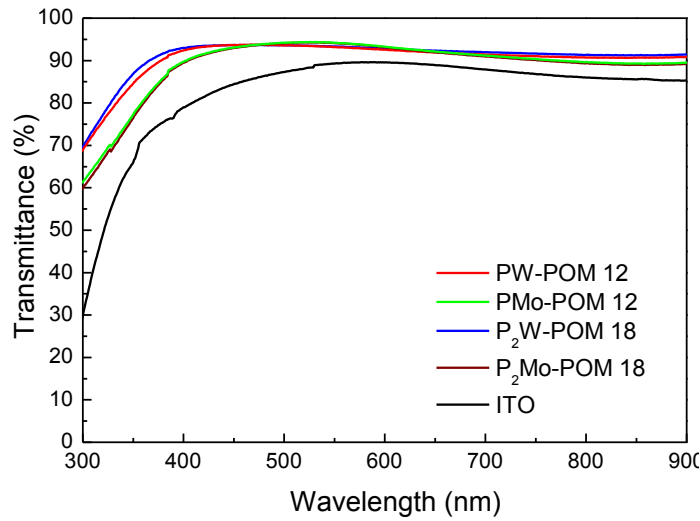
<b>Figure S1</b> AFM topographies of POM films.....	2
<b>Figure S2</b> XRD patterns of PW-POM 12, PMo-POM 12 and P <sub>2</sub> W-POM 18 films.....	3
<b>Figure S3</b> Transmittance spectra of POMs.....	4
<b>Figure S4</b> POMs thickness study: J-V curves of P3HT:PC <sub>71</sub> BM OPVs.....	4
<b>Figure S5</b> UV/vis absorption spectra of 100 nm P3HT:PC <sub>71</sub> BM films on POMs .....	5
<b>Figure S6</b> GIWAXS of 120 nm P3HT:PC <sub>71</sub> BM films on POMs and PEDOT-PSS .....	5
<b>Figure S7</b> UV/vis absorption spectra of POM films .....	6
<b>Figure S8.</b> The energy level diagrams of POMs.....	7
<b>Figure S9</b> UPS Secondary electron cut-off spectrum of ITO.....	7
<b>Figure S10</b> HOMO region of the UPS spectra of thin P3HT films on different POMs.....	8
<b>Figure S11</b> AFM topographies of P3HT:IC <sub>60</sub> BA and P <sub>2</sub> Mo-POM 18 on P3HT:IC <sub>60</sub> BA.....	9
<b>Figure S12</b> Dark J-V curves of front, back and tandem cell .....	9
<b>Figure S13</b> UPS spectrum of a ZnO film.....	10
<b>Figure S14</b> Vacuum level shift at POM/ZnO interface.....	10



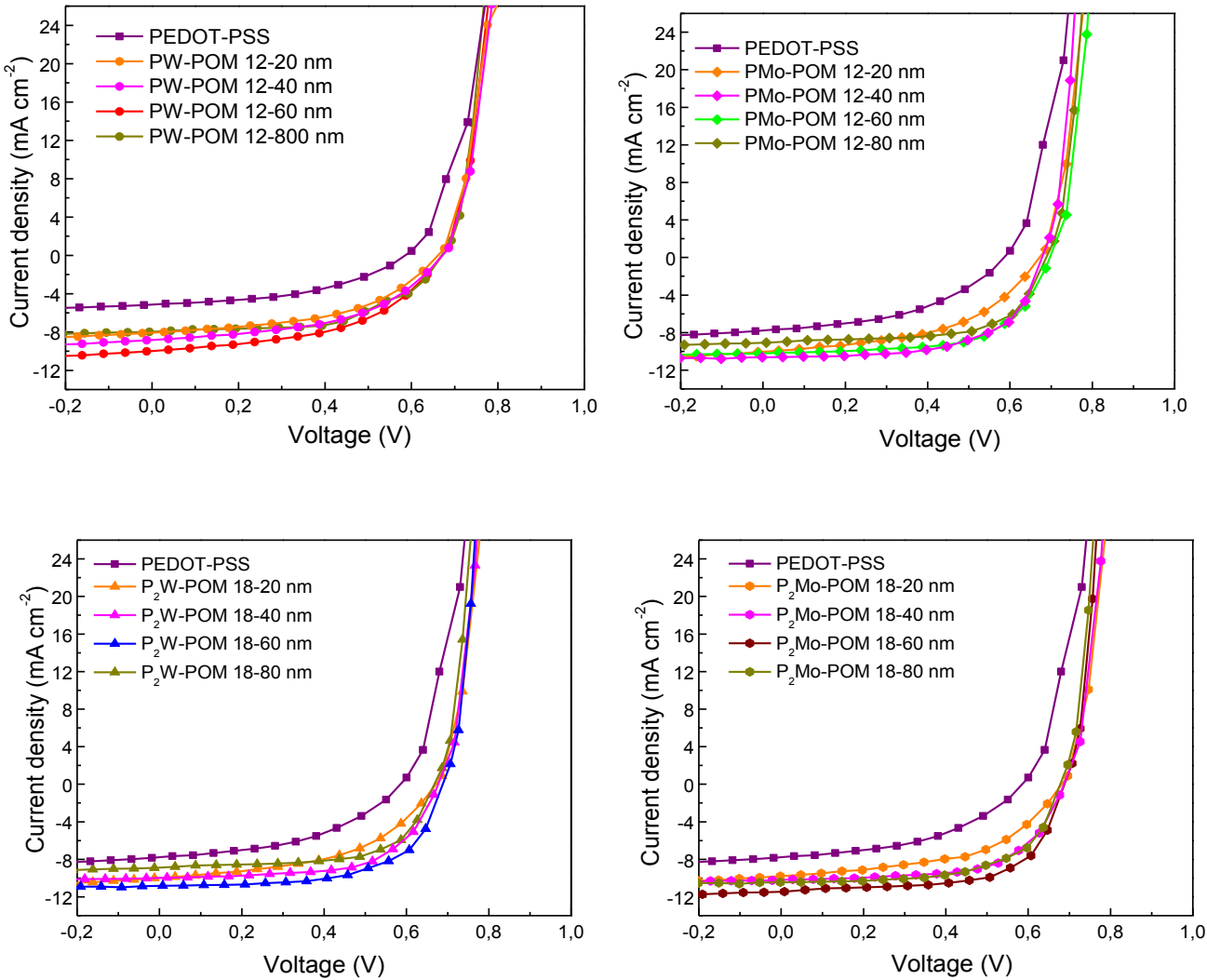
**Figure S1** 3D AFM topographies of PW-POM 12, PMo-POM 12, P<sub>2</sub>W-POM18 and P<sub>2</sub>Mo-POM 18 (from top left clockwise) films with a thickness of 50 nm.



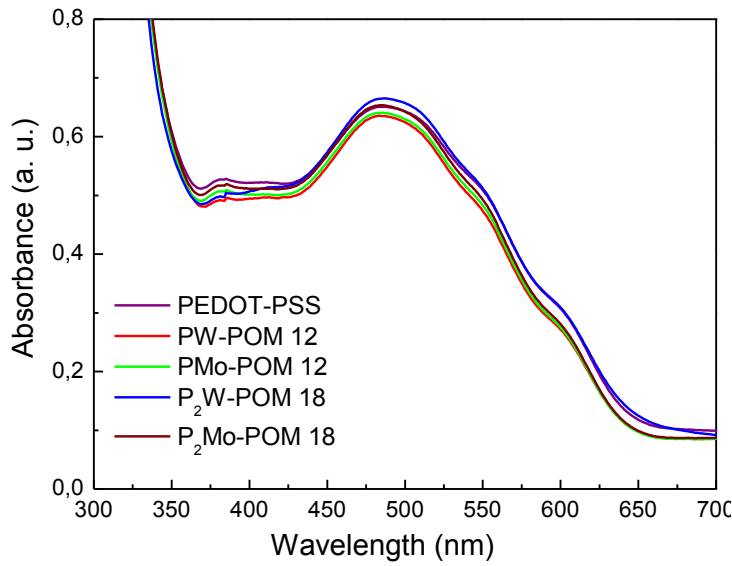
**Figure S2** XRD patterns of different POM films 60 nm thick deposited via spin-coating from methanol solutions without any post deposition annealing treatment.



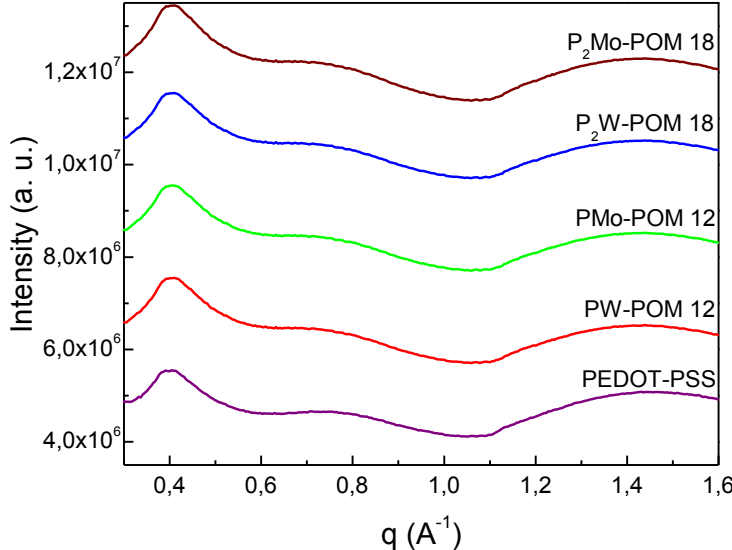
**Figure S3** Transmittance spectra of 60 nm annealing-free POM films deposited on quartz substrates via spin-coating from methanol solutions. The spectrum of ITO on glass is also shown for comparison.



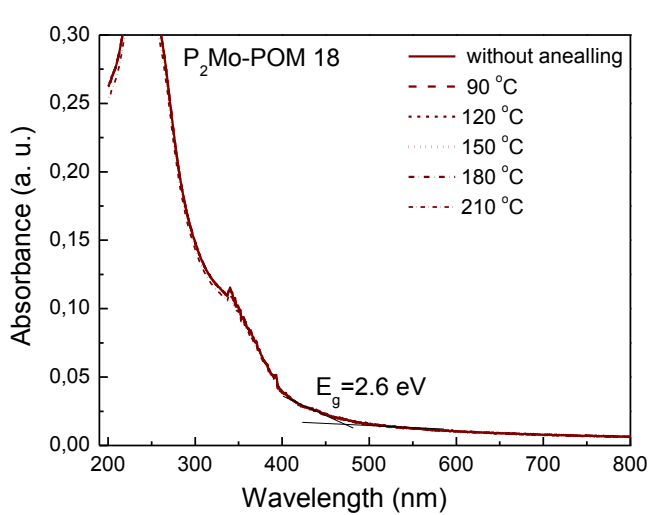
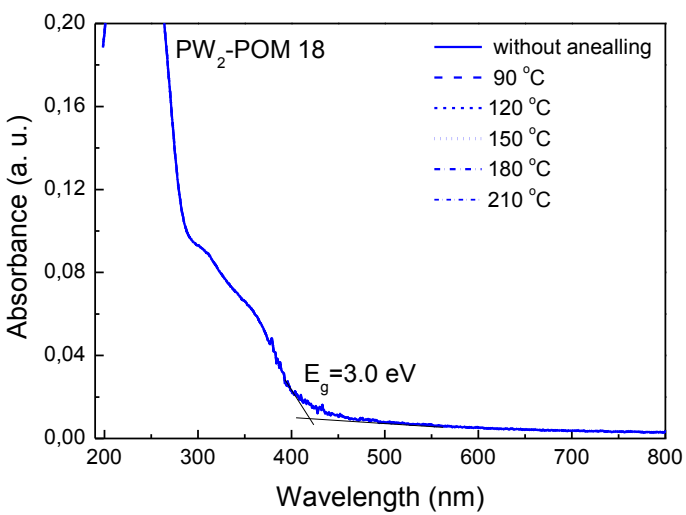
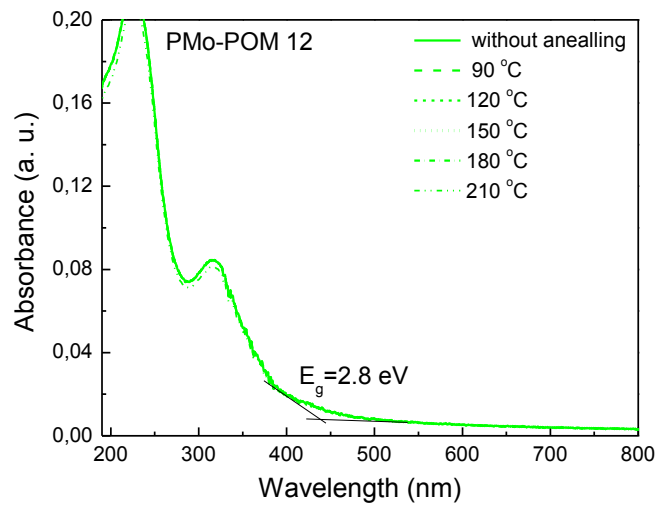
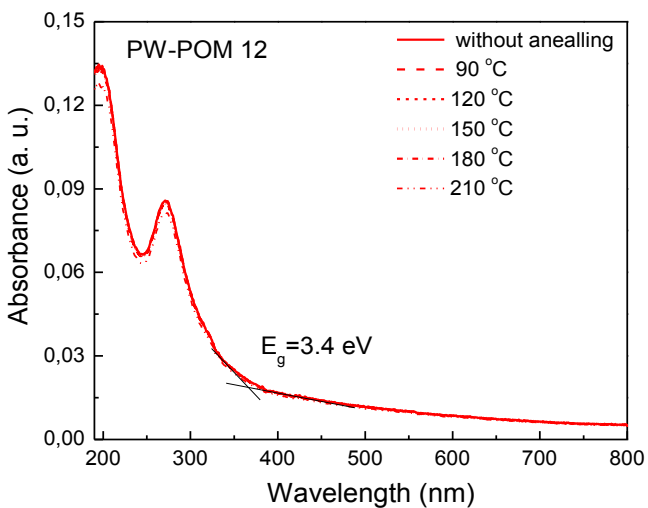
**Figure S4** POMs thickness study: J-V curves of P3HT:PC<sub>71</sub>BM-based OPVs with different thicknesses POM HELs and 40 nm thick ZnO ETL.



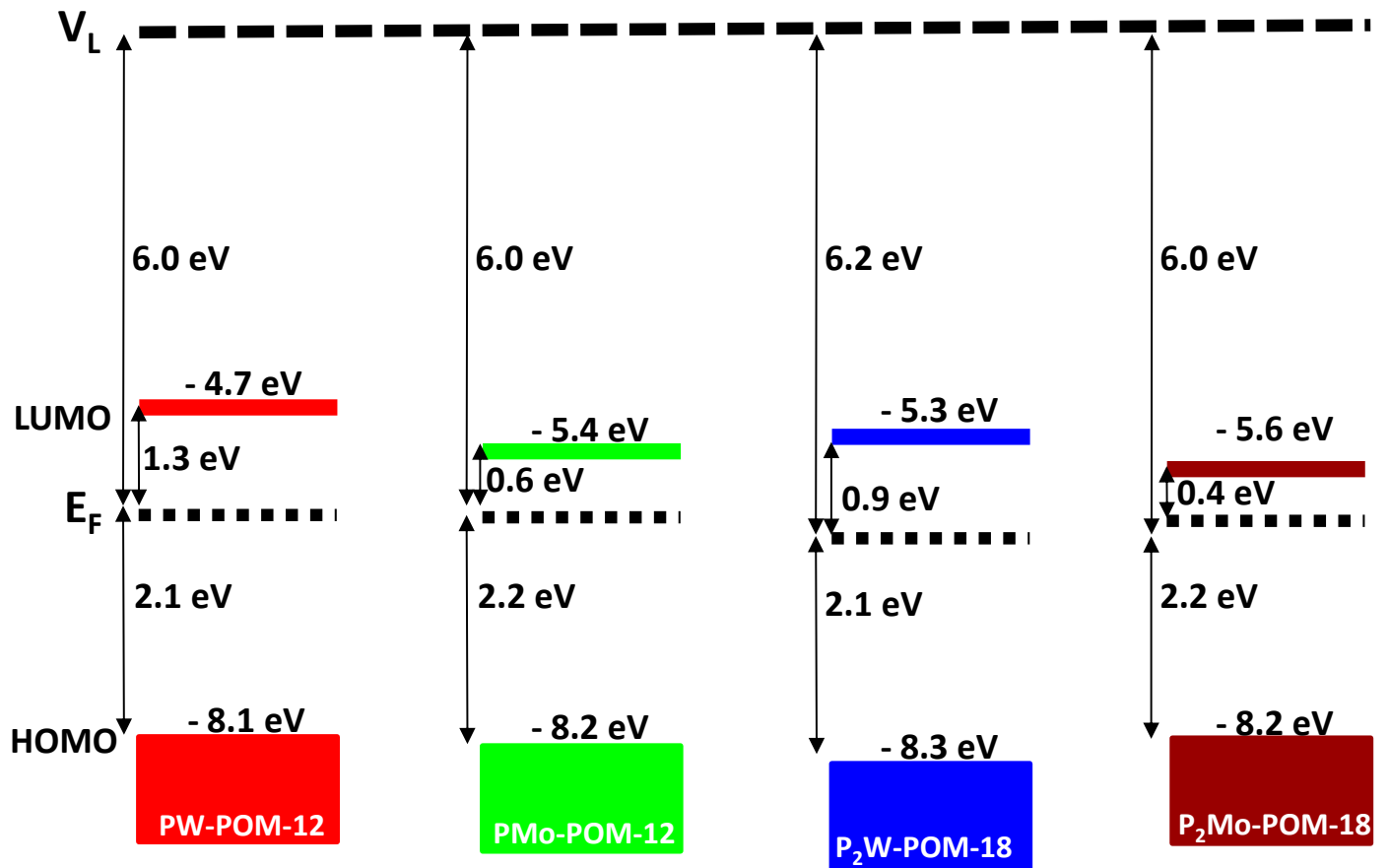
**Figure S5** UV/vis absorption spectra of 120 nm P3HT:PC<sub>71</sub>BM films deposited on different POM layers and on PEDOT-PSS.



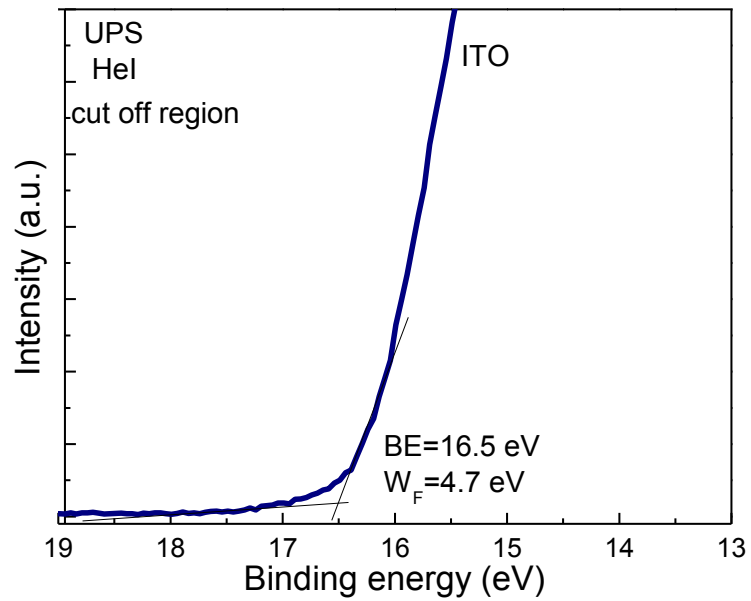
**Figure S6** Grazing incidence X-ray scattering (GIWAXS) of P3HT:PC<sub>71</sub>BM films (as cast, in order to directly probe morphological changes caused by the underlayer) spin-cast from a 18 mg mL<sup>-1</sup> solution in CB deposited onto different layers (on POMs and on PEDOT-PSS). The data are presented with arbitrary units and have been shifted for clarity. The region selected for integration is from  $q = 0.3$  to 1.6 Å<sup>-1</sup>. The peaks observed at  $q \sim 0.39$  Å<sup>-1</sup> and  $\sim 0.75$  Å<sup>-1</sup> are the (100) and (200) peaks of the P3HT component, respectively. The peak observed at  $q \sim 1.42$  Å<sup>-1</sup> originates from crystalline PC<sub>71</sub>BM. (GIWAXS was employed on the BM26B-DUBBLE beamline ( $\lambda = 1.033$  Å, sample-to-detector distance of 2.1 m using a Pilatus 1M 981×1043 pixel detector with pixel size 172 μm) at the European Synchrotron Radiation Facility (ESRF), Grenoble, France).



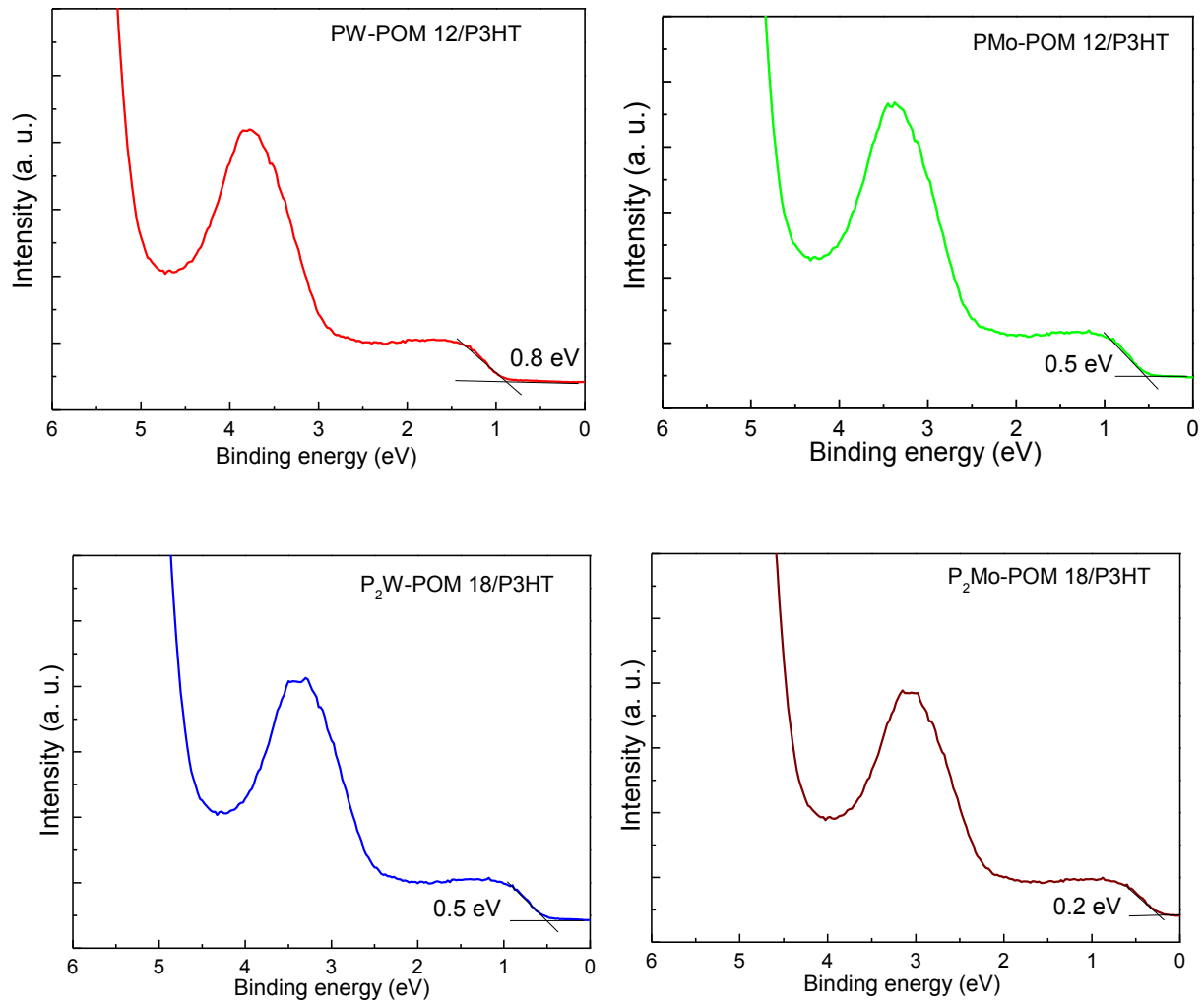
**Figure S7** Absorption spectra of 60 nm POM films deposited on quartz substrates via spin-coating from their methanol solution. Films were either annealing-free for the estimation of their optical energy gap or annealed at elevated temperatures to study their thermal stability.



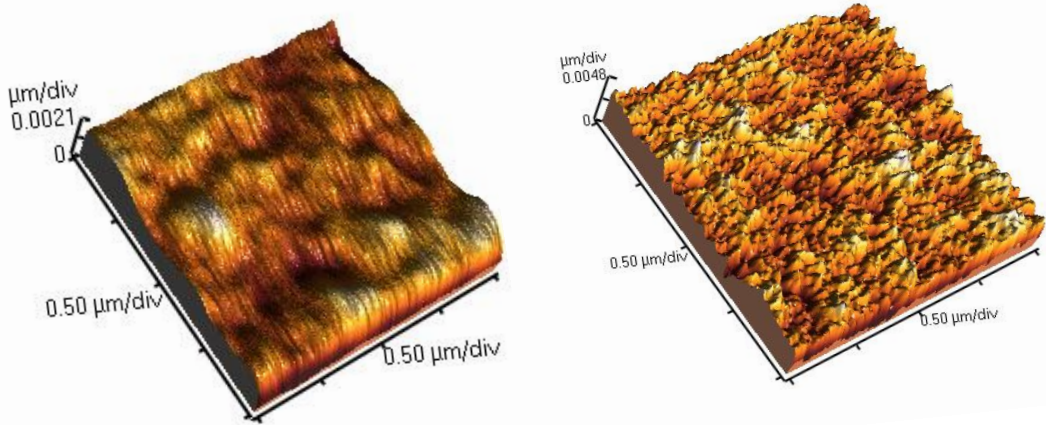
**Figure S8** The energy levels of POMs as derived from the UPS measurements shown in the main manuscript (Figure 4) and the UV-vis absorption measurements shown above (Figure S7). According to the energy levels shown here, POMs are n-type materials since the distance of their Fermi level from their LUMO is smaller compared with the distance from the HOMO.



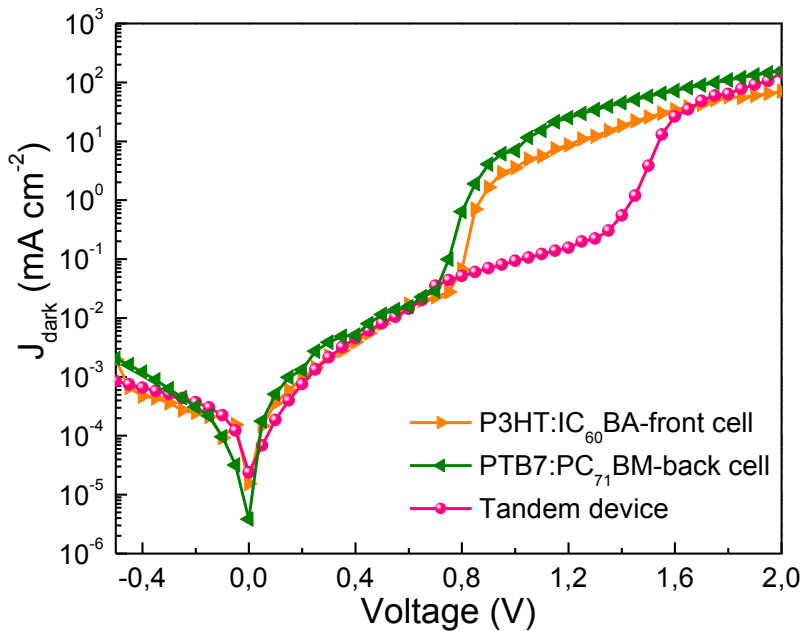
**Figure S9** UPS secondary electron cut-off spectrum of ITO.



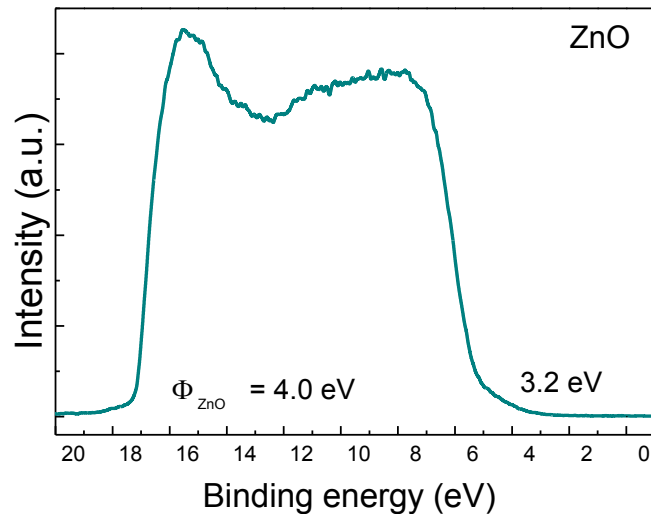
**Figure S10** HOMO region of the UPS spectra of thin (about 3 nm) P3HT films on different POM layers.



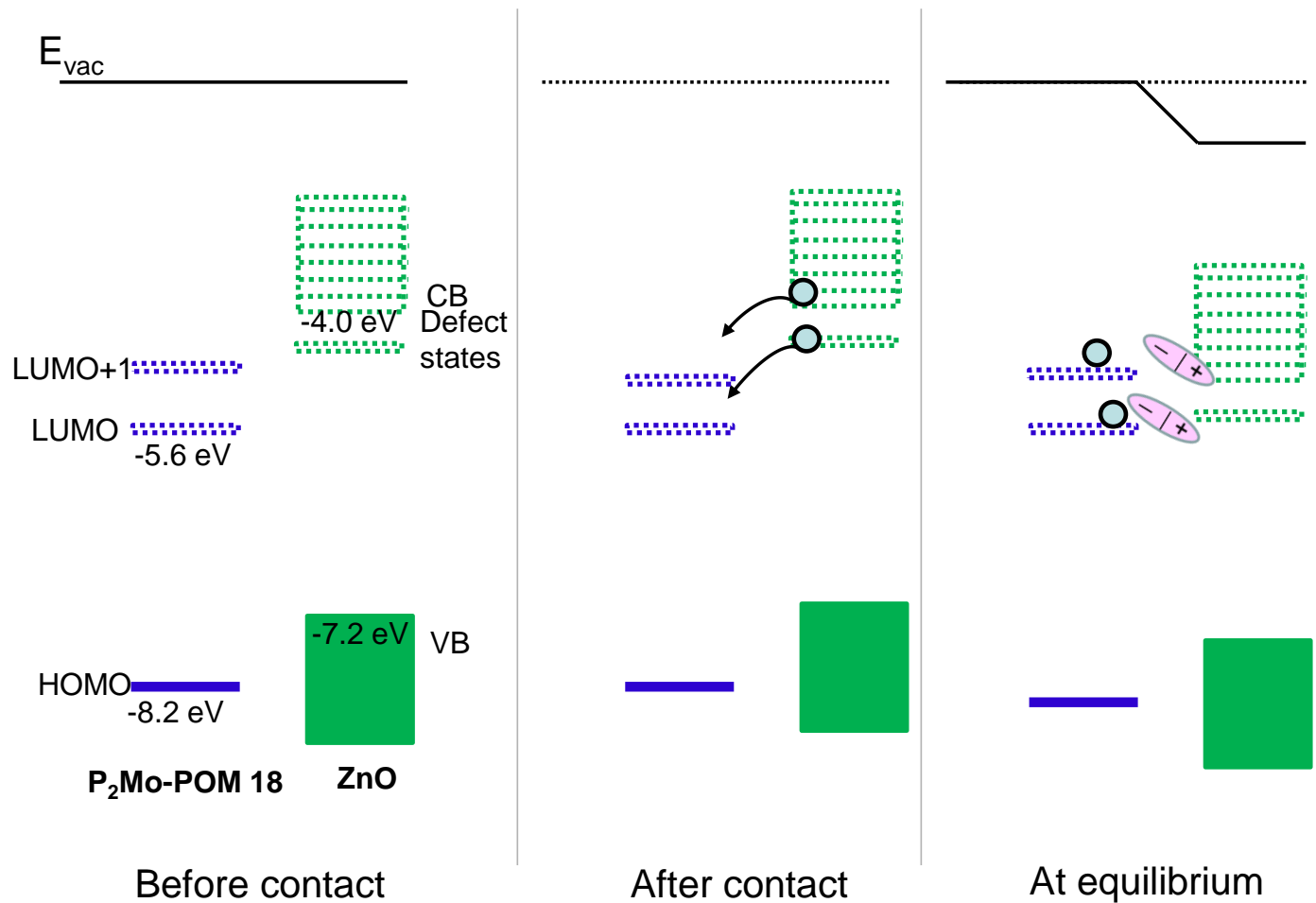
**Figure S11** AFM 3D topographies of P3HT:IC<sub>60</sub>BA (left) and P<sub>2</sub>Mo-POM 18 on P3HT:IC<sub>60</sub>BA (which has been subjected to methanol treatment prior to deposition of the POM layer).



**Figure S12** Dark J-V curves of P3HT:IC<sub>60</sub>BA-front cell, PTB7:PC<sub>71</sub>BM-back cell and Tandem device. The values of series resistance estimated for each cell are: 2.8 Ω cm<sup>2</sup>, 3.3 Ω cm<sup>2</sup> and 8.6 Ω cm<sup>2</sup> for the individual front sub-cell, the back sub-cell and the tandem device, respectively.



**Figure S13** UPS spectrum of 40 nm thick ZnO films.



**S14** Illustration of vacuum level shift *via* the formation of an interfacial dipole due to electron transfer from the conduction band (CB) and/or defect states of ZnO to the LUMO (and/or LUMO+1) level of POM.